

CONCLUSIONS AND SCOPE OF FUTURE WORK

9.1 Summary and conclusions

In the present work development of equivalent circuit models involving Constant Phase angle Elements (CPE) for impedance spectroscopic studies of materials, preparation and characterization of BaTiO₃ ceramics doped with Sr, Fe and Sn by using XRD, SEM, EDS, P-E hysteresis, dielectric measurements as function of temperature and frequency at frequencies below 1 MHz and equivalent circuit modelling, dielectric measurements at microwave frequencies in X-band (8-12 GHz) have been carried out. An attempt has been made for designing of a rectangular dielectric resonator antenna (RDRA) to explore the possibility of technological application of these ceramics. The findings of the studies are summarized below:

(i) Complex plane plots for Impedance (Z), Modulus (M), Admittance (Y), Permittivity (ϵ) for various equivalent circuit models involving constant phase angle elements (CPE), resistances (R 's) and capacitances (C 's) have been simulated for different ratios of the parameters. An indication of presence of certain elements in a possible model to be chosen for a material is obtained by comparing the experimental plots with these simulated ones. A linear portion appearing in the experimental complex plane plot may be considered as a signature of presence of series CPE in the possible model whereas a depressed arc in the Z'' vs Z' or M'' vs M' plot would indicate the presence of CPE connected in parallel. A right shift in Z'' vs Z' plot indicates presence of resistance R in series. When arcs having seemingly three depressed humps, three (R -CPE)

combinations may be considered as a model equivalent circuit. Sometimes peculiar shapes in the complex plane plots are encountered. It has been found that models simulated in this work may be useful where CPE's are included. This hints, greatly facilitate the choice of suitable models by comparing the experimental plots with the simulated ones. This work has given rise to a clear recipe for developing equivalent circuit models for materials and estimating the values of the components. The findings are summarized in Figures 9.1 (a – c) where diagrams at the left hand side represent the shapes of the plots that might arise for a certain material and those at the right side indicate the corresponding models that may be chosen to start with. Choice of a suitable model is a difficult process, becoming more so since several models can be found that show same behavior [Macdoanld et al. (2005); Pandey et al. (1995)]. However, attempts are made to choose a simple equivalent circuit model to start with. This is greatly facilitated by comparing the experimental plots with simulated ones and keeping in mind the charge transfer/polarization processes thought to be possibly present in the system.

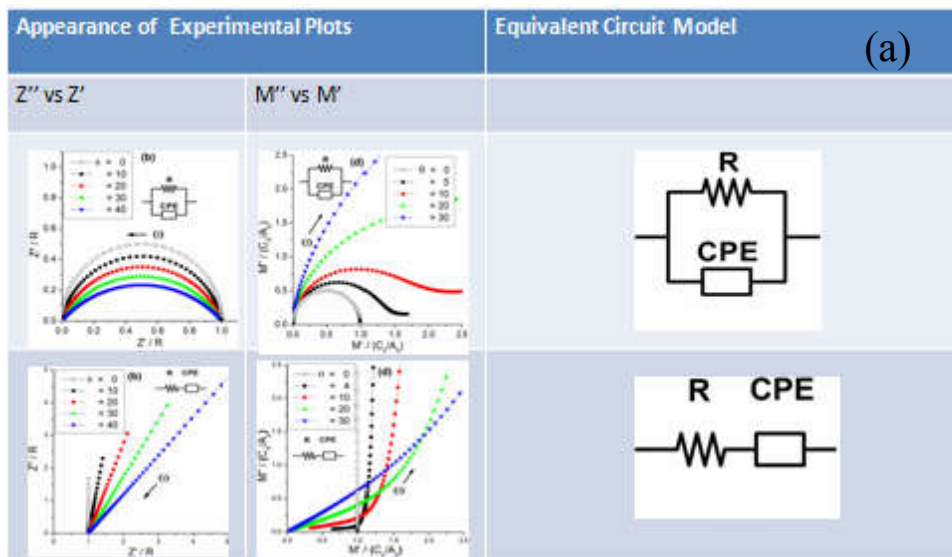


Figure 9.1 : (a)Recipe for obtaining equivalent circuit model involving CPE.

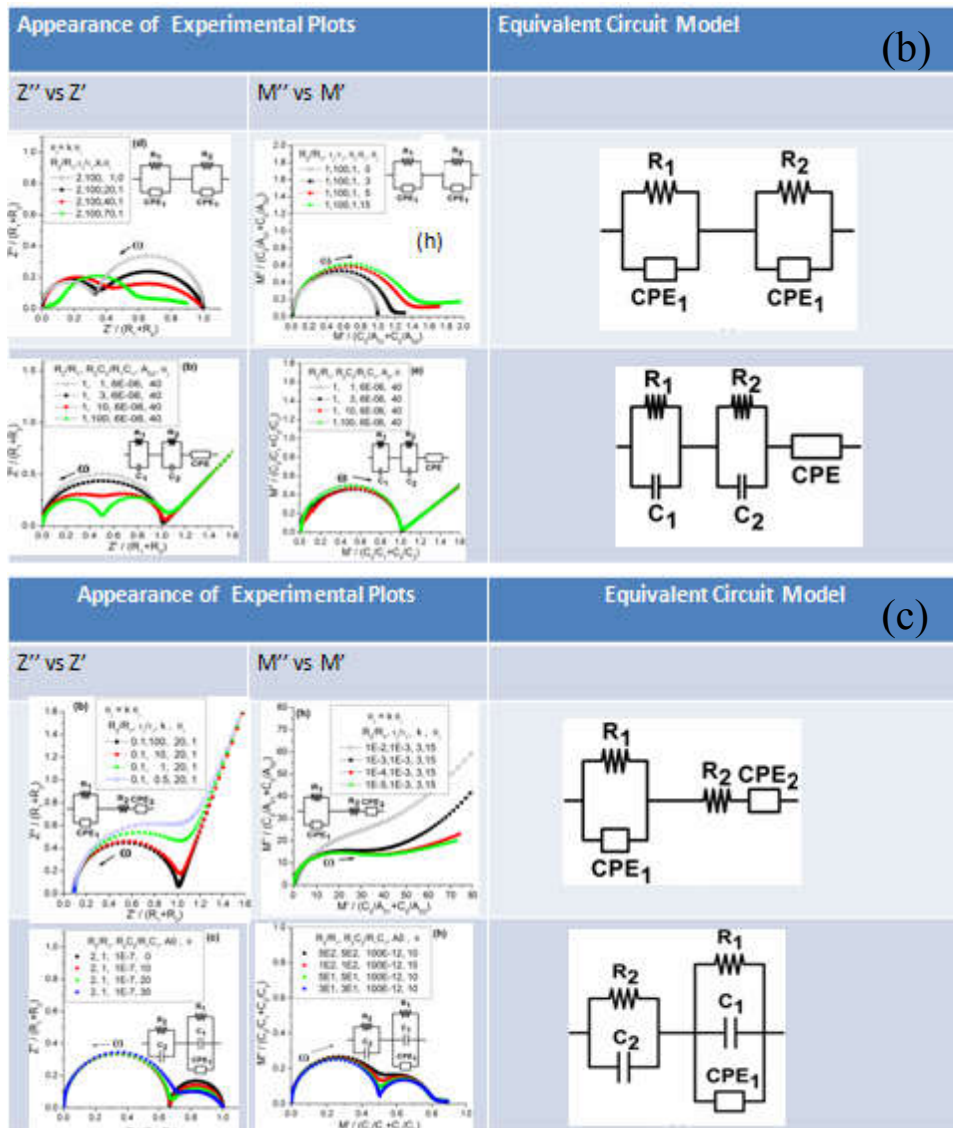


Figure 9.1(contd.): (b,c) Recipe for obtaining equivalent circuit model involving CPE.

(ii) Compositions with $x = 0.15, 0.20, 0.25, 0.30$ and 0.35 in the system $\text{Ba}_{1-x}\text{Sr}_x\text{TiO}_3$ were synthesized using conventional solid state reaction method and characterized by X-Ray Diffraction (XRD), Scanning Electron Microscopy (SEM) and Energy Dispersive Spectroscopy (EDS). Dielectric and impedance measurements were carried out in the temperature range $300\text{K} - 723\text{K}$. As x increases, the temperature of permittivity maxima decreases almost linearly. All the samples exhibit diffuse phase transition. An equivalent circuit model comprising three parallel combinations of resistance and constant phase angle element viz $(R_1 - \text{CPE}_1) - (R_2 - \text{CPE}_2) - (R_3 - \text{CPE}_3)$,

corresponding to grains, grain boundaries and electrode, was developed that represented the data well. Empirical expressions for the values of R_1 , R_2 and R_3 were obtained in terms of temperature and composition. This may be useful in design and simulation studies. Activation energies corresponding to R_1 , R_2 and R_3 are found to vary with x as $(-1.1x + 1.4)$ eV, $(0.4x + 1.0)$ eV and $(0.1x + 0.9)$ eV respectively. Thus as x increases, activation energy for R_1 (i.e. grains) decreases where as for R_2 (i.e. grain boundary) and R_3 (i.e. electrode interface), it increases. P vs. E loop for all the samples indicate a normal ferroelectric behaviour. The values of dielectric permittivity measured in the frequency range 8-12 GHz in the X band of microwaves are around 32, 28, 25, 35 and 42 for x equal to 0.15, 0.20, 0.25 ,0.30 and 0.35 respectively and are almost independent of frequency with the loss being in the range 0.4 to 0.1.

(iii) Compositions with $x = 0.03, 0.05$ and 0.10 were prepared in the system $\text{BaFe}_x\text{Ti}_{1-x}\text{O}_3$ by solid state reaction method and characterized by using XRD, SEM and EDX. It was found that these samples contain both tetragonal and hexagonal phases, the latter increasing as the doping level is raised. Composition with $x=0.03$ exhibits a behavior which mimics relaxor ferroelectrics. Sample with $x=0.05$ shows diffuse phase transition. Contributions of tetragonal and hexagonal phases, grain boundaries and electrode to the overall dielectric behavior have been separated using complex plane modulus analysis and equivalent circuit models representing the data well were developed. The values of dielectric permittivity measured in the frequency range 8-12 GHz in the X band of microwaves are around 16-20 for all the samples and are almost independent of frequency with the loss being around 0.5.

(iv) Compositions with $x = 0.01, 0.10$ and 0.15 were synthesized in the system $\text{BaTi}_{1-x}\text{Sn}_x\text{O}_3$ using conventional solid state method. They were characterized by X-Ray Diffraction (XRD), Scanning Electron Microscopy (SEM) and Energy Dispersive

Spetroscopy (EDS). Tetragonal phase was confirmed for $x = 0.05$ and 0.10 while cubic for $x=0.15$ using Rietveld refinement of the XRD patterns. Dielectric and impedance measurements were carried out in the temperature range $300\text{ K} - 723\text{ K}$ and in the frequency range 1 Hz to 1 MHz . The samples exhibit diffuse phase transition. Equivalent circuit model involving combination of Constant Phase angle Elements (CPE) and resistances (R) was developed which represents the data well. Permittivity is almost independent of frequency and lies in the range $30-45$ for all the samples in the frequency range $8-12\text{ GHz}$. Loss is also almost independent of frequency and lies between $0.10 - 0.30$ for all the samples for this frequency range

(v) Some of the experimental values for the systems studied are summarized in Table 9.1.

(vi) It was found that BTS 15 ($\text{BaTi}_{1-x}\text{Sn}_x\text{O}_3$, $x=0.15$) and BST 35 ($\text{Ba}_{1-x}\text{Sr}_x\text{TiO}_3$, $x=0.35$) have T_c below room temperature and the value of permittivity is about 40 and loss around 0.1 in the X-Band ($8-10\text{ GHz}$). As an attempt to explore possible applications of these, a Rectangular Dielectric Resonator Antenna array was designed and simulated by using HFSS software. The effect of presence of loss in the elements was studied. Design of an aperture coupled RDRA array comprising three elements of permittivity equal to 40 is proposed for microwave X-band operation. When the outer elements are aperture coupled and the middle one is parasitic, the band width increases by 3% (from 1.32 GHz to 1.36 GHz) and gain decreases only by 2.7% (from 5.97 dB to 5.81 dB) as the loss in middle element is increased from 0 to 0.1 keeping the outer elements loss less. The far field pattern remains almost same as loss is increased. These results are promising and indicate that low cost, easily preparable but slightly lossy ($\tan \delta \sim 0.1$) materials, such as $\text{Ba}_{1-x}\text{Sr}_x\text{TiO}_3$ ($x = 0.35$) or BaTi_{1-x}

Sn_xO_3 ($x = 0.15$) ceramics having ϵ_r and $\tan \delta$ around 40 and 0.1 studied in the present work may be used in conjunction with low loss dielectrics in development of antennas by applying the present RDRA design with some trade off with gain.

Table 9.1: Values of room temperature permittivity ϵ'_{RT} , loss, temperature corresponding to maximum permittivity T_m , and diffusiveness parameter γ

| System | Structure at RT | RF Range | | | | Microwave (8-12 GHz) | |
|--|------------------------|-----------------------------|-------------|--------------|----------|----------------------|-------------|
| | | ϵ'_{RT} (1 MHz) | loss | T_m (K) | γ | ϵ'_{RT} | loss |
| $\text{BaFe}_x\text{Ti}_{1-x}\text{O}_3$ | | | | | | | |
| x=0.03 | Tetragonal + Hexagonal | 20 | 0.1 | 377 | 1.22 | 19 | 0.4 |
| x=0.05 | Tetragonal + Hexagonal | 416 | 0.06 | 374 | 1.99 | 18 | 0.5 |
| x=0.10 | Tetragonal + Hexagonal | 66 | 0.06 | - | - | 17 | 0.5 |
| $\text{Ba}_{1-x}\text{Sr}_x\text{TiO}_3$ | | | | | | | |
| x=0.15 | Tetragonal | 1930 | 0.1 | 373 | 1.85 | 31 | 0.3 |
| x=0.20 | Tetragonal | 1690 | 0.03 | 349 | 1.81 | 25 | 0.2 |
| x=0.25 | Tetragonal | 1560 | 0.4 | 323 | 1.28 | 28 | 0.3 |
| x=0.30 | Tetragonal | 3320 | 0.05 | 313 | 1.41 | 37 | 0.2 |
| x=0.35 | Tetragonal | 8260 | 0.1 | - | - | 43 | 0.1 |
| $\text{BaTi}_{1-x}\text{Sn}_x\text{O}_3$ | | | | | | | |
| x=0.05 | Tetragonal | 3843 | 0.2 | 358 | 1.41 | 32 | 0.2 |
| x=0.10 | Tetragonal | 9557 | 0.1 | 323 | 1.60 | 40 | 0.2 |
| x=0.15 | Cubic | 2254 | 0.03 | - | - | 45 | 0.09 |

9.2 Future Scope

The present work was focussed on development of strategies for equivalent circuit modelling of electronic ceramics, preparation and characterization of some doped BaTiO₃ systems and looking for certain designs of rectangular dielectric resonator antenna with a view to explore possible applications of these systems so that such slightly lossy ceramics may also be utilized. The design of rectangular dielectric resonator antenna proposed here is very promising.

Future work on these lines may be taken up where (i) some more equivalent circuit models are studied so as to provide an enriched data base for users (ii) attempts are made to reduce the loss in the BaTiO₃ based systems keeping the values of permittivity high and temperature coefficient of resonant frequency low (iii) designs and fabrication of some more systems to explore further applications.

